Fisheries Research 95 (2009) 55–64

Contents lists available at ScienceDirect

Fisheries Research

journal homepage: www.elsevier.com/locate/fishres

Effects of the gear deployment strategy and current shear on pelagic longline shoaling

Pascal Bach[a,*], Daniel Gaertner[a], Christophe Menkes[b], Evgeny Romanov[a], Paulo Travassos[c]

[a] IRD, Centre de Recherche Halieutique, Avenue Jean Monnet, BP 171, 34203 Sète Cedex, France
[b] Centre IRD, Anse Vata, BP A5, 98848 Nouméa Cédex, Nouvelle Calédonie, France
[c] UFRPE – LEMAR/DEPAq - Recife – PE - CEP 52.171-900, Brazil

ARTICLE INFO

Article history:
Received 3 April 2008
Received in revised form 5 July 2008
Accepted 22 July 2008

Keywords:
Monofilament pelagic longline
Temperature-depth recorders
Maximum fishing depth
Sag ratio
Generalized additive model (GAM)
Generalized linear model (GLM)

ABSTRACT

Historical longline catch per unit effort (CPUE) constitutes the major time series used in tuna stock assessment to follow the trend in abundance since the beginning of the large-scale tuna fisheries. The efficiency and species composition of a longline fishing operations essentially depends on the overlap in the vertical and spatial distribution between hooks and species habitat. Longline catchability depends on the vertical distribution of hooks and the aim of our paper was to analyse principal factors affecting the deviation of observed longline hook depths from predicted values. Since observed hook depth is usually shallower than predicted, this deviation is called longline shoaling. We evaluate the accuracy of hook depth distribution estimated from a theoretical catenary model commonly used in longline CPUE standardizations. Temperature-depth recorders (TDRs) were deployed on baskets of a monitored longline. Mainline shapes and maximum fishing depths were similar to gear configurations commonly used to target both yellowfin and bigeye tuna by commercial longliners in the central part of the South Pacific Ocean. Our working hypothesis assumes that the maximum fishing depth reached by the mainline depends on the gear configuration (sag ratio, mainline length per basket), the fishing tactics (bearing of the setting) and environmental variables characterizing water mass dynamics (wind stress, current velocity and shear). Based on generalized additive models (GAMs) simple transformations are proposed to account for the non-linearity between the shoaling and explanatory variables. Then, generalized linear models (GLMs) were fit to model the effects of explanatory variables on the longline shoaling. Results indicated that the shoaling (absolute as well as relative) was significantly influenced by (1) the shape of the mainline (i.e., the tangential angle), which is the strongest predictor, and (2) the current shear and the direction of setting. Geometric forcing (i.e. transverse versus in-line) between the environment and the longline set is shown for the first time from *in situ* experimental fishing data. Results suggest that a catenary model that does not take these factors into consideration provides a biased estimate of the vertical distribution of hooks and must be used with caution in CPUEs standardization methods. Since catchability varies in time and space we discuss how suitable data could be routinely collected onboard commercial fishing vessels in order to estimate longline catchability for stock assessments.

© 2008 Elsevier B.V. All rights reserved.

1. Introduction

Stock assessment procedures for many tropical large pelagic fish such as yellowfin tuna (*Thunnus albacares*), bigeye tuna (*Thunnus obesus*), and albacore (*Thunnus alalunga*) are commonly based on longline fisheries data analysis, in which catch per unit effort (CPUE) is usually standardized to account for changes over time in fishing strategies to provide refined indices of population abundance (or availability). However, the hypothesis that considers catch rates as an index of abundance, and the ability to adequately standardize catch rates, has been the subject of much debate (Richards and Schnute, 1986; Maunder et al., 2006a,b). For a passive longline fishing, this hypothesis is further complicated by the fact that longline catchability is influenced by a number of factors related to gear configuration (Ward and Hindmarsh, 2007). Thus while variables such as area, year, and season are commonly considered in CPUE standardization, many others factors such as bait, fishing materials, day vs. night fishing period, soaking time, and fishing depth which are known to influence CPUE and are often not taken into account in such standardizations (Boggs, 1992; Bjordal and Lokkeborg, 1996; Hinton and Nakano, 1996; Nakano et al., 1997; Satoh et al., 1990; Takeuchi, 2001;

* Corresponding author.
E-mail address: bach@ird.fr (P. Bach).

0165-7836/$ – see front matter © 2008 Elsevier B.V. All rights reserved.
doi:10.1016/j.fishres.2008.07.009

Nomenclature

BS	bearing of the setting
DS	direction of the setting
DBF	horizontal distance between floats
DMB	depth at the middle position of the mainline basket
GDS	gear deployment strategy
HBF	number of hooks between floats
LB	length of the branchline
LF	length of the floatline
LLBF	mainline length between floats
MAD	median value of depth mean values recorded on several baskets of a given set
MFD	predicted maximum fishing depth according to the catenary algorithm
SR	sag ratio = ratio between DBF and LLBF
TDR	temperature depth recorder
φ	angle between the horizontal and tangential line of the mainline

Bigelow et al., 2002; Ward et al., 2004; Ward and Myers, 2005). Among these factors, longline fishing depth (and the corresponding hook depth distribution) directly affects the longline catchability as defined as "a measure of the interaction between the resource abundance and the fishing effort" (Arreguin-Sanchez, 1996). As such, in many analyses the number of hooks between floats (HBF) is commonly used as a proxy indicator of the maximum fishing depth, however, some studies suggest that this proxy should be used cautiously (Bach et al., 2006). More recently, a new approach known as "habitat-based-standardization" (Hinton and Nakano, 1996; Bigelow et al., 2002; Campbell, 2004) and "statistical-habitat based standardization" (Maunder et al., 2006a,b) has been developed. Longline effective effort is measured as the overlap between hook depth distributions and the availability distribution of the fish population in the water column. Finally, Ward and Myers (2005) estimate catchability related to depth to correct abundance indices for variations in longline depth. However, the robustness of both these empirical and deterministic standardization methods concerns the estimation of the hook depth distribution.

To improve our knowledge of longline impacts on large pelagic resources either targeted or untargeted we have to answer the question "how deep are the longline hooks according to both a gear deployment strategy (GDS) and oceanographic conditions? Unfortunately, few studies have focused on this question despite its continual interest since the early years of longline fisheries (Yoshihara, 1951, 1954; Kuznetsov, 1969; Gerasimov, 1971; Boggs, 1992; Hinton and Nakano, 1996). Some studies have inferred hook depths by assuming a catenary shape for the mainline (Yoshihara, 1951, 1954; Kuznetsov, 1969; Gerasimov, 1971; Suzuki et al., 1977; Hanamoto, 1987; Gong et al., 1989; Nakano et al., 1997). Knowing the gear configuration (mainly the 'sag ratio' and the length of the mainline between buoys), the catenary geometry leads to an estimation hook depths (Yoshihara, 1951, 1954; Kuznetsov, 1969) when effects of external factors (such as currents) on the gear are not significant. However, a number of longline fishing trials have deployed instruments such as micro-bathythermographs (micro-BTs), depth recorders (DRs) and temperature-depth recorders (TDRs) and have shown that the assumed depths according to catenary geometry are often not obtained (Nishi, 1990; Boggs, 1992; Mizuno et al., 1997, 1998; Campbell, 1997; Okazaki et al., 1997; Bach et al., 2003; Bigelow et al., 2006; Miyamoto et al., 2006). For these studies, when theoretical maximum fishing depths and maximum recorded depths have been compared, predicted catenary depths were usually deeper than observed depths.

Interaction of longline gear with the oceanic environment, generally with oceanic currents shoal the mainline and branchlines and prevent them from reaching their maximum depths. Shoaling of the mainline has been observed to vary between 11% and 46% depending on fishing grounds and fishing periods (Nishi, 1990; Boggs, 1992). Furthermore, by coupling longline depth monitoring and vertical current profiles, Mizuno et al. (1998) clearly showed variations of the sag ratio parameter during a single longline set. Recently, longline shape simulations using numerical methods have also shown sag ratio variations and the shoaling of the mainline subjected to current effects (Lee et al., 2005; Miyamoto et al., 2006). Sag ratio is one of the key parameters defining mainline shape and depth and can be monitored by deploying GPS buoys (Mizuno et al., 1998; Okamura et al., 1998; Miyamoto et al., 2006). However, as GPS buoys are not deployed very often during longline fishing operations the direct effect of sag ratio variations on differences between predicted and observed depths is usually not taken into account in longline depth analysis.

In this study, we analyze mainline depths recorded at the mid-point of the longline basket during monitored longline fishing experiments carried on in oceanic waters surrounding French Polynesia in the central part of the South Pacific (Bertrand et al., 2002; Bach et al., 2003). The monitored set used a traditional "deep gear" configuration. Within-set records are compared and the relevance of the catenary formula is explored. Differences between both observed and predicted maximum fishing depths of the mainline, known as longline shoaling, are modelled according to both mesoscale oceanographic descriptors and variables describing both the gear configuration and the fishing operation. Finally, longline set level operational data that should be collected routinely by commercial vessels in order to estimate the maximum fishing depth are discussed.

2. Data and methods

2.1. The monitored longline

The fishing gear consisted of a nylon monofilament (3.5-mm diameter) mainline stored on a drum and deployed by a line shooter. During fishing operations a transmitter buoy was attached at each end of the mainline. At a regular time interval, 20-m polypropylene floatlines was attached to the mainline to maintain the gear at the sea surface. Monofilament branch lines of 2-mm diameter and 12-m long were attached at a constant time interval within for a given set. A section of the longline delimited by two floats is traditionally named "basket" (Fig. 1).

For each longline set of about 20–26 baskets with 25 hooks each, at least 50% of baskets were equipped with temperature-depth recorders (TDR, model LL 600 from Micrel company). TDRs were programmed to record fishing depth once per minute. Each TDR was positioned with two snaps at the mid-point on the basket mainline.

2.2. Fishing operations

Longline fishing experiments were carried out on board the IRD R/V "*Alis*" from July 1995 to August 1997. The 142 fishing operations considered in this study were made in the north-eastern part of the French Polynesia EEZ between latitudes 5°S to 20°S and longitudes 134°W to 153°W. In general objectives of the longline monitoring were to deploy the gear during the day and in a manner that the effective fishing depths overlapped

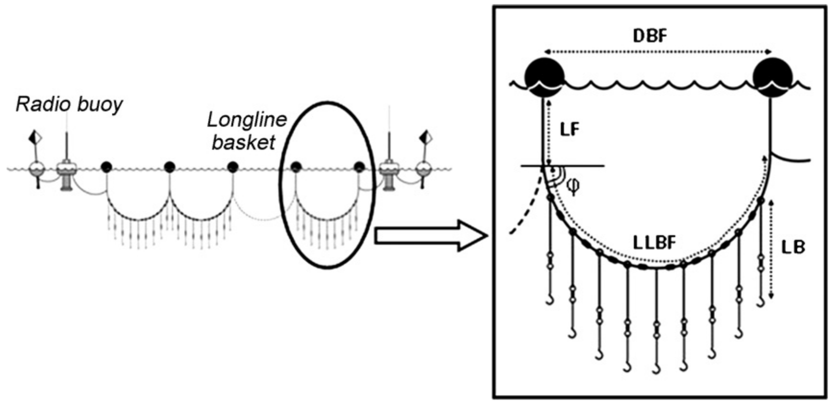

Fig. 1. A pelagic longline with details on the configuration of a single basket unit and annotations used in the text. DBF is the horizontal distance between two floats, LLBF is the mainline length between two floats, LF is the length of the floatline, LB is the length of the branchline and φ is the angle between the horizontal and the tangential line of the mainline.

the vertical habitat of large pelagic fishes which ranged from the sea surface temperature to the 7 °C isotherm (Bach et al., 2003).

For each fishing trial, data that characterize the setting procedure were collected. For a given set, the number of hooks between floats (HBF), the time interval between attaching hooks, the vessel speed and the shooter speed controlled with a tachometer were uniform while setting (i.e. all baskets within a longline set were homogeneous). Each longline was deployed in a straight line and the positions and times of the start and the end of the longline setting and the hauling were recorded to calculate the great circle distance of the longline set. The horizontal distance between floats (DBF, mean value = 804 ± 92 m) was estimated by the ratio between the great circle distance of the set and the number of baskets. The setting time of the set was calculated by the product between the total number of intervals between hooks or between floats and hooks (i.e. corresponds to the formulae number of hooks + number of floats − 1) multiplied by the beeper time interval which was 14 s in general. Total length of the mainline deployed for a set corresponds to the product between the setting time and the shooter speed. Mainline length between floats (LLBF, mean value = 1298 ± 106 m) was then estimated by the ratio between the mainline length for the set and the number of baskets. The mainline concavity per basket commonly named the sag ratio (SR) was calculated as the ratio between DBF (numerator) and LLBF (denominator).

2.3. Selection of depth data recorded at the mid-point on the basket mainline

The deepest point of the mainline is theoretically at the middle position of the mainline basket (DMB, Fig. 1) and its depth depends on the gear configuration and the gear deployment strategy (GDS) as well as environmental forces affecting longline gear. However, DMB can be greatly modified by fish capture irrespective if the catch occurs near the middle position of the line or not (Okazaki et al., 1997; Fig. 2). Thus the catch of a fish represents a disruptive factor in the general context of the longline behaviour, which is the purpose of this study. Consequently, all TDRs data obtained on baskets with catches were removed from the analysis. We selected fishing operations where at least three TDRs records were available for non-consecutive baskets. The dataset contained 142 fishing operations (∼426 maximum fishing depth profiles) based on the three TDR criterion.

2.4. Maximum fishing depth at the set level

The vertical movement of the middle position of the mainline is characterized by three major periods: the sinking period while setting, the rising period while hauling and an intermediate period generally named the fishing time when the longline is at settled depths. The duration of the sinking period depends on the maximum depth targeted, longline gear configuration (i.e. monofilament or multifilament, weight of mainline and branchlines, presence of additional weights on gear, type and condition of bait (frozen or thawed), etc.) and the environment. For example, in our study, for a DMB equal to 400 m, the duration of sinking was ranged between 30 min and 1.5 h. The end of the sinking period was defined at the time when 5 consecutive values of the relative variation of the depth were less than 1%. The beginning of the rising period corresponded to the time when the basket is retrieved and was indicated by a vertical line on the fishing depth profile. The intermediate period located between these two time values was the period of interest. Depth values considered in this study corresponded to depths recorded during this period. For these depth series, respective mean values are calculated (i.e. 3 mean depth values are calculated for each set). In order to eliminate the within set variability of mean values in the statistical analysis of the longline shoaling, we consider the median of the mean values. In the following, the acronym MAD corresponds to the median value of the depth mean values. The MAD value is considered as representative of maximum fishing depths of the three different baskets for a given set.

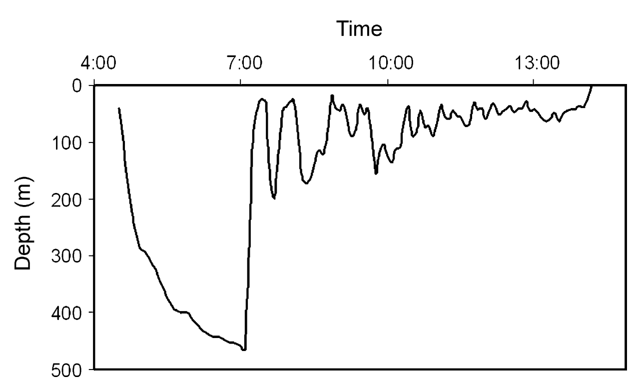

Fig. 2. Time series of the recorded depths of the mainline indicating large movements due to the capture of a swordfish (50 kg) on a hook attached just adjacent to the temperature-depth recorder.

2.5. Theoretical maximum fishing depth

The theoretical depth of a hook j can be estimated by using the catenary geometry formulae (Yoshihara, 1951, 1954; Suzuki et al., 1977):

$$D_{\mathrm{j}} = \mathrm{LF} + \mathrm{LB} + \left(\frac{\mathrm{LLBF}}{2}\right) \times \left\{(1+\cot^2\varphi)^{1/2} - \left[\left(1-\left(\frac{2\mathrm{j}}{N}\right)\right)^2 + \cot^2\varphi\right]^{1/2}\right\} \quad (1)$$

where D_{j} is the depth of the jth hook, LF is the length of the floatline, LB is the length of the branchline, LLBF is the length of the mainline between two consecutive floats (basket), N is HBF + 1, j is the jth hook from the floatline, φ is the angle between the horizontal and the tangential line to the mainline (Fig. 1).

In general, the variable used to describe the shape of the mainline is not the angle φ but the sag ratio (SR) defined as the ratio between the horizontal distance between floats (DBF) and the length of the mainline between floats (LLBF). Yoshihara's formula (1954) calculates SR knowing φ:

$$\mathrm{SR} = \frac{\mathrm{DBF}}{\mathrm{LLBF}} = (\cot\varphi) \times \ln\left[\left(\tan\left(\frac{45^\circ + \varphi}{2}\right)\right)\right] \quad (2)$$

As data collected in the field allow the SR to be estimated directly, the angle φ was solved by iteration by using Eq. (2). This angle was then used in Eq. (1) to calculate the maximum fishing depth:

$$\mathrm{MFD} = \mathrm{LF} + \mathrm{LB} + \left(\frac{\mathrm{LLBF}}{2}\right) \times \{(1+\cot^2\varphi)^{1/2} - (\cot^2\varphi)^{1/2}\} \quad (3)$$

where MFD is the predicted maximum fishing depth according to the catenary algorithm.

2.6. Environment covariates

Differences between observed and predicted depths of the mainline and hooks are mainly due to effects of the oceanographic environment on the longline. Wind intensity, current velocity and direction and vertical shear are commonly mentioned as exogenous factors responsible for longline shape deformation (Boggs, 1992; Mizuno et al., 1998; Lee et al., 2005; Bigelow et al., 2006; Miyamoto et al., 2006). As *in situ* environment data were not collected during the fishing trials, vertical profiles of current velocities (u = zonal current, v = meridional current) were obtained from the LODYC (Madec et al., 1999) general circulation model. A full description and validation of the dynamics of that model can be found in Menkes et al. (2006). The domain spans the tropical Pacific between 120°E and 75°W, 30°N and 30°S. The model has a 1° zonal resolution and a meridional resolution varying from 0.5° between 5°N and 5°S to 2° at the northern and southern boundaries. There are 25 levels (with a 10 m resolution down to 150 m and 1.5 h time step). After 3 years of spin-up using climatological winds, the model is run for the 1992–1998 period, but results were analyzed for 1995–1997. Five-day outputs were used in the present study.

The date of each longline set and location (the latter was defined as the midpoint of the longline setting positions) were used to reference the corresponding current profile outputs.

Current profiles data were used to estimate current profile velocities, $\mathrm{VC_i}$:

$$\mathrm{VC}_i = [(u_i)^2 + (v_i)^2]^{1/2}$$

where u: zonal current, v: meridional current, i: layer.

For each current profile, we consider: $\mathrm{VC_{ml}}$ = the current velocity in the mixed layer defined as the mean of current velocities observed in the 10 initial layers between layers 5 m and 95 m.

Current shear between the surface and thermocline is one of the major oceanographic dynamic factors mentioned as responsible for longline shoaling (Bigelow et al., 2002, 2006). Non-transformed vertical shear was used in the analysis:

$$W = \left\{ \frac{\sum_{i=1}^{I}[((u_i+1-u_i)/(z_i+1-z_i))^2 + ((v_i+1-v_i)/(z_i+1-z_i))^2]^{1/2} \times (z_i+1-z_i)}{\sum_{i=1}^{I}(z_i+1-z_i)} \right\}$$

where u_i is the zonal current of the layer i, v_i is the meridional current of the layer i, z_i is the depth of the layer i. The vertical shear W for each fishing set was estimated for the water column between the surface (layer 5 m) to the layer 490 m (i.e. 19 layers) which overlaps the majority of maximum fishing depth experiments considered in the study.

2.7. Statistical modelling of longline shoaling

Accounting for factors from both the gear deployment strategy (GDS) and environment that affect longline hook depths was conducted with generalized additive models (GAM) and generalized linear models (GLM). These methods were used to analyze the deformation of the longline as measured by the absolute shoaling and the relative shoaling:

$$\text{Absolute shoaling (m)} = \mathrm{MFD} - \mathrm{MAD}$$
$$\text{Relative shoaling (\%)} = 100 \times (1 - \mathrm{MAD}/\mathrm{MFD})$$

where MFD is the maximum fishing depth according to catenary algorithms and MAD is the median of observed mean depths at the set level.

To facilitate comparisons with previous studies which focused on the analysis of bias associated with the use of the predicted catenary depth in the hooks depth distribution, the level of shoaling and relative shoaling were modelled separately in a GLM framework as a function of variables characterizing (i) the GDS (the length of the mainline between floats = LLBF, the direction of the setting = DS and the tangential angle of the mainline = φ) and (ii) the vertical shear of current components = shear.

The direction of the setting (DS) was introduced to test the potential effect of the direction of the environmental forcing in relation to the longline. DS was defined as the bearing of the longline set and ranged from 0° (i.e. the longline is parallel to meridians) to 90° (i.e. the longline is parallel to parallel lines).

Three principal environmental factors are usually considered to explain depth deviations from predicted catenary depths: current velocity, shear and wind stress (Bigelow et al., 2006). However, an exploratory analysis of our data showed that two of these covariates estimated by the ocean model, were highly correlated (Pearson's coefficient r = 0.84 between the shear and the average current velocity in the mixed layer). Consequently, to prevent potential colinearity with the current shear in the GLM analysis, the current velocity in the mixed layer was not used in the present analysis.

Generalized Additive Models (GAM) extend the range of application of Generalized Linear Models (GLM) by allowing nonparametric smoothers to capture the shape of relations between response and the explanatory variables without restricting these relationships to a linear form. In complement with GLM analyses, GAMs can be considered as an exploratory and visualization tool highlighting the unexpected influence of some variables on the distribution of the response (Venables and Ripley, 2002). However, we

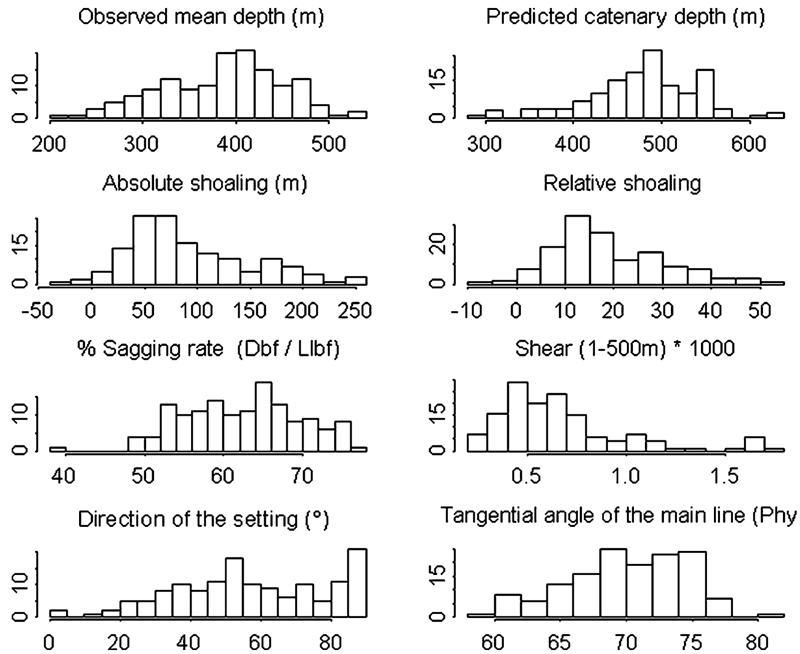

Fig. 3. Frequency distributions of observed and catenary depths, shoaling levels, and associated gear setting and current shear variables for all sets included in the analyses.

prefer to use GAM outputs to suggest parametric transformations of the variables that are substantively interpretable (i.e. when the relationship is as linear as possible) rather than to use directly the transformations estimated in their raw form. If the plots of the GAM transformations are roughly continuous and monotonic we focus on simple power transformations as approximations to the GAM transformations. On the other hand, if the plot shows discontinuities, this may suggest that the variable should be categorized as separate regimes (Hoeting et al., 1996).

The objective in model building is to reach a trade-off between the extremes of under fitting the data (too little structure, which means large bias) and over fitting the data (too many parameters, hence large variance). The search for the number of optimal parameters that minimizes both functions of bias and variance may be done with an Akaike's information criterion (AIC), which is widely used as an objective means of model selection from a set of candidate models (Lebreton et al., 1992; Anderson et al., 1994). The model with the smallest AIC is defined as the most parsimonious model. Once an adequate model is selected, the neighbouring nested models are checked with likelihood ratio test to detect whether important factors (including interactions) are necessary. Regression diagnostics were used to judge the goodness-of-fit of the model. These included an overall measure of fit assessed by the "pseudo $R^{2''}$ and conventional diagnostic plots to identify outliers and influential observations (Venables and Ripley, 2002).

3. Results

3.1. Candidate variables and dependant variables

Fig. 3 depicts the frequency distributions of the dependant variables (both absolute and relative shoaling) and each of the candidate predictors. The monitored longline deployed during this study had a constant 25 hooks between floats. The LLBF ranged from 931 m to 1560 m (average: 1298 m). The DBF ranged between 532 m to 1035 m (average: 804 m). The minimum and maximum values of the sag ratio distribution were 39% and 76.7%, respectively (average: 62.3%). For 73% of the sets the direction of setting ranged from 45° to 90° while 27% ranged between 0° and 45° has an average value of 58° (Fig. 3).

3.2. Predicted catenary and observed fishing depths

Predicted catenary MFD values ranged from 296 m to 630 m. The mean value was 477 m and 75% of predicted values were deeper than 447 m. These deep values were mainly the consequence of a low sag ratio due to considerable slack in the mainline. Distributions of predicted catenary and observed depths showed a quite similar shape (cf. Fig. 3); however, compared to predicted catenary depth, observed depth was generally 100 m shallower (minimum and maximum values were 218 m and 523 m, respectively and the mean value was 385 m). The absolute shoaling distribution ranged from −27 m to 255 m with a mean value of 92 m, whereas the relative shoaling distribution ranged from −7.4% and 51.3% around a mean of ~19% (Fig. 3).

3.3. Modelling the relative shoaling of the longline

To achieve homogeneity of variance the relative shoaling of the longline was transformed as:

$$\text{tRShoaling} = \sqrt{\text{RShoaling} + 8}$$

The constant was added in the transformation formulae in order to avoid negative values. The distribution of the transformed values is plotted in Fig. 4.

Our modelling approach consisted of a trade-off between (i) the best fit by using spline smoothers and featuring automatic selection of smoothing parameters from the data and (ii) a simple linear model by restricting all of the partial-regression functions to be linear. With this consideration in mind, first a suitable transformation for all the candidate variables was performed within a GAM framework. These candidate variables were current shear, the direction of the setting, the shape of the mainline (tangential angle φ), catenary depth and the length of the mainline between floats (LLBF). Among

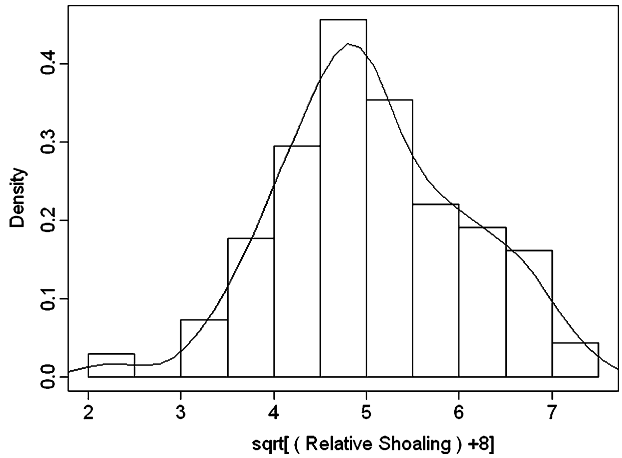

Fig. 4. Frequency distribution of the transformed relative shoaling variable (tRShoaling = $\sqrt{\text{RShoaling} + 8}$).

these variables, only the current shear, direction of the setting and the shape of the mainline were significant (Table 1A). Results of the GAM derived effects of these three variables on the transformed relative shoaling are presented in Fig. 5. The shape of the mainline (tangential angle φ) exhibited a roughly positive linear pattern and was used without transformation in the different candidate GLMs. The plot of the smooth term for the variable "Shear" was roughly monotonous. However, the trend of this relationship suggests that shoaling and shear are inversely related. Consequently, a reciprocal transformation 1/shear was applied for the GLM modeling. For the effects of the variable "setting direction" on the relative shoaling, GAM outputs suggested an absence of effects for direction ranging from 0° to 45° and a positive linear effect at greater angle. Thus, a categorized variable named "CDirection" was proposed with CDirection = 45° if the direction of the setting is under or equal to 45° otherwise CDirection = the recorded direction (a sensibility analysis confirmed that 45° represents the best threshold value).

The smallest AIC, and as a consequence, the most parsimonious model, was obtained by using a non-parametric smoother in each term (i.e., the GAM):

$$\text{tRShoaling} = \beta_0 + s(\text{Shear}) + s(\text{Direction}) + s(\varphi)$$

The simple generalized linear model below appears as a reasonable trade-off with the most of the optimal explained variance (R^2 = 0.169 compared to 0.21) captured:

$$\text{tRShoaling} = \beta_0 + \beta_1\,\text{Shear}^{-1} + \beta_2\,\text{CDirection} + \beta_3\varphi$$

Table 1
Generalized linear models and associated statistics for describing the transformed longline shoaling as a function of the intercept, current shear (Shear), the direction of the setting (untransformed = Direction, and categorized at 45° = CDirection) and the tangential angle of the main line (φ)

A. Relative longline shoaling

Model ($y = [RShoaling+8]^{0.5}$)	Res. dev.	d.f	AIC	Pseudo-R^2
y = *inter.* + s(*Shear*) + s(Direction) + s(φ)	106.327	123.002	-25.47	0.210
y = *inter.* + *Shear*$^{-1}$ + *CDirection* + φ	111.895	132	-18.53	0.169
y = *inter.* + *Shear*$^{-1}$ + *CDirection*+ φ + *Shear*$^{-1}$: φ	111.583	131	-16.91	0.171
y = *inter.* + *Shear*$^{-1}$ + *CDirection*+ φ + *Shear*$^{-1}$:*CDirection*	111.699	131	-16.77	0.170
y = *inter.* + *Shear* + *Direction* + φ	113.814	132	-16.22	0.155
Null Deviance (*intercept only*):	134.616	135		

B. Absolute longline shoaling

Model ($y = [Shoaling+50]^{0.5}$)	Res. dev.	d.f	AIC	Pseudo-R^2
y = *inter.* + s(*Shear*) + s(*Direction*) + s(φ)	467.409	123.002	175.90	0.330
y = *inter.* + *Shear*$^{-1}$ + *CDirection* + φ	492.393	132	182.98	0.295
y = *inter.* + *Shear*$^{-1}$ + *CDirection* + φ + *Shear*$^{-1}$:*CDirection*	491.413	131	184.71	0.296
y = *inter.* + *Shear*$^{-1}$ + *CDirection* + φ + *Shear*$^{-1}$: φ	491.867	131	184.84	0.295
y = *inter.* + *Shear* + *Direction* + φ	504.466	132	186.27	0.277
Null Deviance (*intercept only*):	698.000	135		

Models have been ranked from best to worst according to the Akaike weights.
Res. dev.: Residual deviance, d.f.: degree of freedom. The model corresponding to the best trade-off is highlighted.

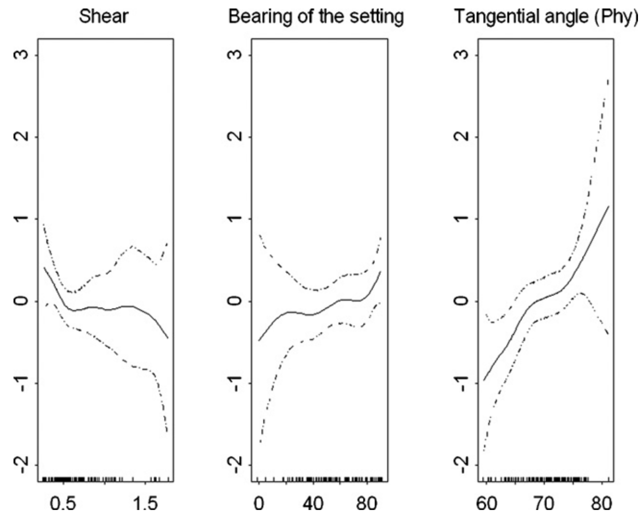

Fig. 5. Generalized additive model (GAM) derived relationships between current shear, direction of the setting and shape of the mainline (tangential angle φ) and the transformed relative longline shoaling. *Dashed lines correspond to the 95% confidence intervals*.

The analysis of the deviance table (Table 1A) suggests that compared to the model built with the untransformed explanatory variables, the model supporting simple transformations significantly improves the fit of the response variable. The presence of interactions Shear^{-1}: φ and Shear^{-1}: CDirection were not supported by the data. The tangential angle φ is the strongest and the most consistent predictor ($P < 0.001$). This variable explains 72.2% of the pseudo R^2 of the parsimonious model (Table 2A). Moreover, we can note that the term Shear^{-1} appears to be of borderline significance ($p = 0.051$) while CDirection does not have any effect on tRShoaling ($p = 0.076$) at the 5% level.

3.4. Modeling the absolute shoaling of the longline

For the absolute shoaling the transformation presented below was applied:

$$\text{tShoaling} = \sqrt{\text{Shoaling} + 50}$$

The frequency distribution of the transformed values is displayed in Fig. 6.

Table 2
Parameter estimates for the model describing the transformed longline shoaling as a function of the intercept (β_0), reciprocal transformation of the shear (Shear^{-1}), categorized direction of the setting (CDirection) and the tangential angle (φ) of the mainline

Model $y = \beta_0 + \beta_1$ Shear^{-1} + β_2 CDirection + $\beta_3\varphi$				
Parameter	Estimate	S.E.	*P*-value	%var. expl.
(A) Relative longline shoaling				
β_0	−1.169	1.259	0.353	
β_1 (Shear^{-1})	0.201	0.103	0.051	14.2
$\beta2$ (CDirection)	0.009	0.005	0.076	11.8
β_3 (φ)	0.076	0.017	<0.001	72.2
(B) Absolute longline shoaling				
β_0	−7.671	2.641	0.004	
β_1 (Shear^{-1})	0.464	0.216	0.032	8.5
β_2 (CDirection)	0.022	0.010	0.032	8.5
$\beta3$ (φ)	0.244	0.036	<0.001	81.7

P-values are derived from the Wald statistic. The percentage of variance explained (%var. expl.) is based on the relative difference between the pseudo R^2 value form the selected model, and the pseudo R^2 from the same model without the corresponding explanatory factor.

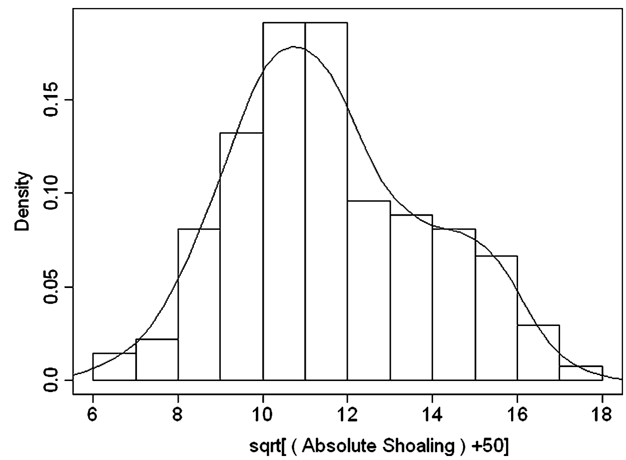

Fig. 6. Frequency distribution of the transformed absolute shoaling variable (tShoaling = $\sqrt{\text{Shoaling} + 50}$).

A suitable transformation for all the candidate variables was performed in a GAM framework. The significant candidate variables in this model are similar to those selected for the relative shoaling analysis. GAM results for these three variables on the transformed absolute shoaling are presented in Fig. 7. The optimal transformations provided by a GAM produced a R^2 of 0.33 (Table 1B). It should be stressed that relationships between the smooth term and the observed values of the different candidate variables exhibit similar shapes to those observed previously.

As seen previously for the relative shoaling, the model supporting simple transformations significantly improves significantly the fit of the absolute shoaling. Moreover, interactions between Shear^{-1} and the other covariates remain non-significant. A model formulation similar to these retained for the GLM of the relative shoaling appears as a reasonable trade-off:

$$t\text{Shoaling} = \beta_0 + \beta_1 \text{Shear}^{-1} + \beta_2 \text{CDirection} + \beta_3 \varphi,$$

Most of the explained variance has been captured by this simple model ($R^2 = 0.295$ compared to 0.33). Parameter estimates for this model are presented in Table 2B. The candidate variable φ charac-

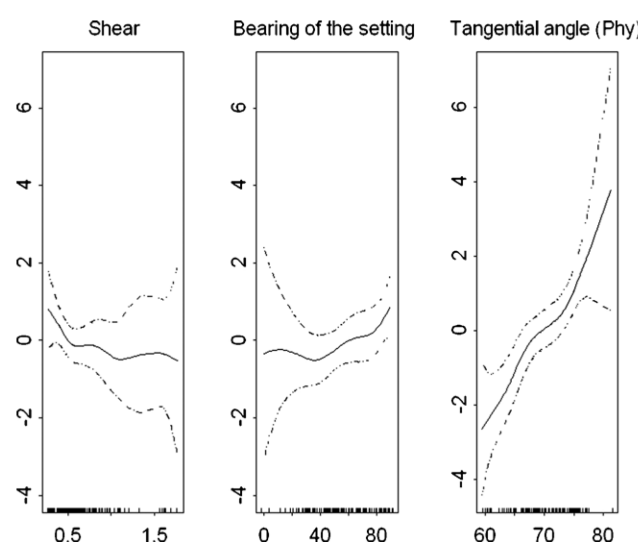

Fig. 7. Generalized additive model (GAM) derived relationships between current shear, direction of the setting and shape of the mainline (tangential angle φ) and the transformed absolute longline shoaling. *Dashed lines correspond to the 95% confidence intervals*.

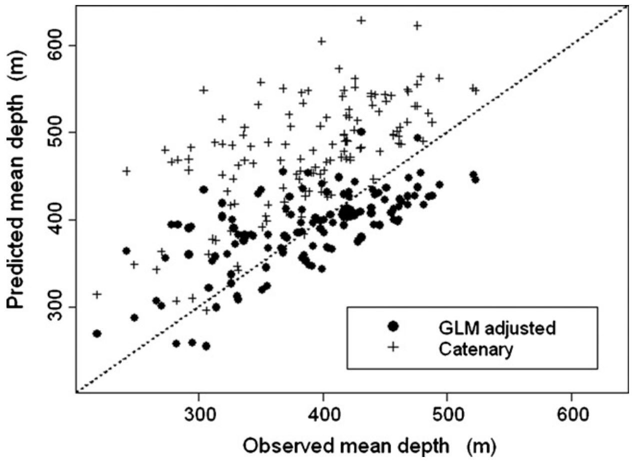

Fig. 8. Comparison of observed depth, catenary curve depth estimates, and modelled depth based on absolute shoaling from a generalized linear model (GLM).

terizing the shape of the mainline is the most consistent predictor ($P < 0.001$). This variable explains 81.7% of the pseudo R^2 of the parsimonious model (Table 2B). The reciprocal transformation of the shear and the categorized transformation of the direction of the setting are of secondary importance to explain the variability of the shoaling (for each of them, $P = 0.032$). The sign of the parameters in the model for each predictor is positive. Finally, it is important to highlight that all the models fit for absolute shoaling have the highest explanatory ability (pseudo-R^2) than predictive models of the relative shoaling.

Catenary depths, observed depths and modelled depths estimated from this last model are displayed in Fig. 8. Modelled depths are relatively well distributed along the 45° line, especially when compared to catenary depths, which had considerably higher values than observed depths. However, it should be noted that for the largest differences between catenary and the observed depths occur at extreme situations where the GLM estimations have less accuracy.

4. Discussion

This study supports the results of previous studies that the monofilament longline maximum fishing depth and the related hook depth distribution cannot be directly inferred from catenary geometry (Mizuno et al., 1997, 1998; Lee et al., 2005; Bigelow et al., 2006). In this context our findings also provide some insights into identifying some of the factors which influence the magnitude of longline shoaling.

All data analyzed in the present study were obtained from monitored longline sets. This allowed information related to the gear deployment strategy (GDS, i.e., the distance between buoys, the length of the mainline between buoys, the tangential angle of the mainline as well as the direction of the setting) to be collected as accurately as possible. Moreover, multiple TDRs were attached to the middle position of the mainline between two adjacent floats to collect information on the deepest depth.

However, for a number of reasons the assumption that the midpoint of a basket represents the deepest point of the mainline may not hold true: (1) the presence of a caught fish may have a great influence on the depth of the line (Okazaki et al., 1997), (2) the observed maximum fishing depth for a longline configuration may differ between baskets (as observed in this study), and (3) the middle position on the mainline between two floats may not always represent the deepest point of the longline (Mizuno et al., 1997, 1998). For all of these reasons, depth was recorded only from baskets without a catch. Furthermore, the median of the depths recorded on three non-consecutive baskets was taken as being representative of the maximum depths attained by mainline within a given set.

Longline shoaling has been observed in both multifilament longline (Kuznetsov, 1969; Gerasimov, 1971; Hanamoto, 1974) and monofilament longline (Nishi, 1990; Boggs, 1992; Okazaki et al., 1997; Mizuno et al., 1997, 1998; Bigelow et al., 2006) trials. It is one of the principal factors, which introduces uncertainties in the standardization of pelagic longline CPUEs (Hinton and Nakano, 1996; Bigelow et al., 2002; Campbell, 2004; Ward and Myers, 2005), but few studies have attempted to model the resulting longline deformation. Bigelow et al. (2006) analysed the relative shoaling of the monofilament pelagic longline from TDR monitoring in the commercial Hawaii-based longline fishery, and Miyamoto et al. (2006) analysed both shape and depths variations of the mainline in real-time by using an ultrasonic positioning system. Environmental effects on the longline have also been studied using numerical simulation approaches (Offcoast Inc., 1997; Lee et al., 2005). All these studies confirmed the deformation of longline shape under the influence of environmental factors. Moreover, simulation studies clearly demonstrated that for a given gear configuration the intensity of the deformation depends on the position of the line compared to the current direction (Lee et al., 2005).

Two major conclusions can be drawn from our analysis. First, in terms of significance of the predictor variables used in the statistical models (GAMs and GLMs) as well as in the explanatory ability to predict the level of shoaling, it appears modelling of absolute longline shoaling is more appropriate than relative shoaling. Second, despite shear having a significant effect, two factors characterizing the GDS: the shape of the mainline and the direction of the setting, are also seen to significantly influence shoaling. The longline shape (i.e. the sag ratio) was found to have the most explanatory ability and the most consistent predictor in GLMs.

It is a common practice to express longline shoaling in term of a percentage. Boggs (1992) estimated the average percentage of the mainline shoaling at 46% and 32%, respectively for two survey periods. From TDRs deployed on the mainline aboard longline commercial vessels Bigelow et al. (2006) estimated mean shoaling values at about 35% for tuna sets (deep longline configuration) and at 55% for swordfish sets (shallow longline configuration). In the present study, the relative longline shoaling values for deep longline sets ranged from −7% to 51.3%, with an average at 19%. Absolute longline shoaling values varied from −27 m to 255 m around a mean of 92 m.

The better explanatory power of models fitted to the absolute shoaling compared to relative shoaling suggests that the mainline deformation due to currents is independent of the maximum fishing depth (i.e. a given absolute shoaling corresponds to a given current shear). For others fishing trials, an increase in the shoaling percentage with depth has been observed for hook depths (Mizuno et al., 1998). Unfortunately the shoaling observed at the deepest point of the mainline cannot be extrapolated from these observations the internal forces which work at different points of the fishing gear (attachment locations of hooks along the mainline for example) being different. Additional data coming from both monitored experiments at sea and numerical simulation approaches are still needed to select the more consistent indicator of the longline shoaling: absolute or relative.

It must be stressed that for the two distinct formulations of the shoaling (i.e. absolute and relative), the respective final models embedded the same three explanatory variables: the shear, the mainline shape (i.e. the tangential angle in our models) and the direction of the setting. Thus, this is the first time that the effect of GDS on the longline shoaling has been statistically demonstrated from modelling *in situ* data. It must be noted that shoaling differences due to the direction of the longline relative to current directions were shown in simulation studies (Offcoast Inc., 1997 in Bigelow et al., 2006; Lee et al., 2005).

Regarding the general pattern of the shoaling variations, it can be seen that shoaling increases when the tangential angle and direction of the setting increase. In contrast, an inverse relationship is observed with the shear such that a larger shear produces a smaller difference between the catenary and observed depths.

This result differs from that reported by Bigelow et al. (2006) where increasing shoaling due to shear effects was observed though mainly for shallow sets rather than deep sets and for fishing operations located within the Equatorial Undercurrent area (where high horizontal shear was observed; Mizuno et al., 1998). In this study area, shear is characterized by low values and current velocities are dominated by zonal rather than meridional currents. Moreover, there may be s spatio-temporal mismatch between longline monitoring and current data because the environmental covariates corresponded to outputs of a coupled ocean-atmosphere model with a spatial-temporal resolution of about 1° and 5 days. Differences between estimated and *in situ* shear conditions are likely to exist, particularly at small scales. This aspect could be one explanation of the discrepancy between GLM estimations and large values between observed and respective catenary depths. With these considerations in mind it can reasonably be assumed that the relationship between the shoaling and the shear might be a consequence of (i) the discrepancy between oceanographic model outputs and actual oceanographic conditions and (ii) the deformation of the mainline due to others factors related to the setting tactic and their interactions with current conditions. Based on justified hypotheses, different authors pointed out that ocean currents in a transverse direction to the longline could generate a greater shoaling than parallel forcing (Lee et al., 2005; Bigelow et al., 2006). In this study, the trend of the relationship between the mainline shoaling and the setting direction supported this assumption. As previously explained the direction of the setting was defined as a categorical variable in GLMs with a threshold value at 45°. Below this threshold the direction of the setting was fixed at 45° otherwise the direction of the setting was set to its observed value (i.e. following GAM results). Our findings suggest that shoaling increases with an increasing transverse direction of the longline. In the present study, such an effect can be detected only for angles of the direction of the setting (DS) above 45°. On the other hand, no shoaling effect was shown for in-line forcing (i.e. $0° \leq DS < 45°$). In such a situation the deformation of the mainline during the soaking time principally corresponded to an increase of the sag ratio. An evidence of this deformation is proved by the negative values observed for the shoaling (due to variations of the sag ratio during the soak time). Unfortunately, GPS buoys which are needed to quantify this phenomenon (Mizuno et al., 1998) were not available during our fishing experiments.

The tangential angle φ appeared as the most consistent shoaling predictor. Shoaling and φ depicted the same pattern of variations. A positive relationship between shoaling and the shape of the mainline has been suggested earlier (Mizuno et al., 1998) and this is the first time that this relationship has been demonstrated by modelling. Notice that this effect is probably underestimated due to the potential change of the sag ratio during the soaking time. Consequently a combined effect between oceanographic factors and the direction of setting may induce large deformations of the longline shape. Unfortunately we were not able to evaluate whether these deformations may compensate for the degree of shoaling due to shear or not. All of these results suggest that important interactions should exist between the different predictors considered in our model; however, inclusion of interactions in the modelling framework was not supported by the data.

Some authors have noted that the robustness of longline CPUE standardizations could be related to the adequacy of the gear models (Goodyear et al., 2003; Bigelow et al., 2006). Knowledge of the longline behaviour during the set is still too poorly understood to be integrated successfully into the standardization of longline fishing effort. To improve this situation, attention must be focused on data describing the gear deployment strategy, specifically the sag ratio (i.e. the length of the mainline per basket and the distance between floats) and the direction of the setting. For this purpose some of the required information collected during observer programs should be extended to commercial logbooks and recorded on a continuous basis by fishermen (Bach et al., 2006).

Moreover, several studies with multifilament longlines (Kuznetsov, 1969; Gerasimov, 1971) suggests that shoaling of the multifilament gears which has been replaced by monofilament longlines in the most of longline operations by the 1990s, was lower. This suggests that additional information is required to assist in the analysis of historical CPUE data.

Given these conclusions, CPUE standardization would be improved by a research program devoted to the analysis of the fishing gear behaviour in different oceans (i.e., how the gear is fishing). Materials and technological deployments (e.g., depth recorders or temperature-depth recorders, Acoustic Doppler Current Profiler, tachometer, portable GPS, GPS buoys) useful in collecting *in situ* gear behaviour and oceanographic data should be implemented. Finally, acquisition of these data could be incorporated into the large number of sophisticated statistical approaches now available for standardizing CPUE (Maunder and Punt, 2004).

Acknowledgements

Data collection was conducted within the ECOTAP program with the financial support of the Government of French Polynesia. We thank the officers and crew of the IRD R.V. “Alis” for their cooperation and professionalism. We thank also all partners and participants involved in this program. Two referees provided ideas and plenty of editorial suggestions that improved our manuscript. This work was developed in part within the framework of the research program “Performance of Longline Catchability Models in Assessments of Pacific Highly Migratory Species” within the Pelagic Fisheries Research Program (PFRP). We thank all the participants in the first meeting on “Pelagic longline catch rate standardization” held in Hawaii from 12th to 16th of February 2007 for their relevant remarks and discussions. In particular, we are very grateful to K. Bigelow (NMFS, Hawaii) for his encouragement for exploring this type of approach.

References

Anderson, D.R., Burnham, K.P., White, G.C., 1994. AIC model selection in overdispersed capture recapture data. Ecology 75 (6), 1780–1793.
Arreguin-Sanchez, F., 1996. Catchability: a key parameter for fish stock assessment. Rev. Fish Biol. Fish. 6, 221–242.
Bach, P., Dagorn, L., Bertrand, A., Josse, E., Misselis, C., 2003. Acoustic telemetry versus monitored longline fishing for studying the vertical distribution of pelagic fish: bigeye tuna (*Thunnus obesus*) in French Polynesia. Fish. Res. 60, 281–292.
Bach, P., Travassos, P., Gaertner, D., 2006. Why the number of hooks per basket (HPB) is not a good proxy indicator of the maximum fishing depth in drifting longline fisheries? Col. Vol. Sci. Pap. ICCAT 59 (2), 701–715.
Bertrand, A., Josse, E., Bach, P., Gros, P., Dagorn, L., 2002. Hydrological and trophic characteristics of tuna habitat: consequences on tuna distribution and longline catchability. Can. J. Fish. Aquat. Sci. 59, 1002–1013.
Bigelow, K.A., Hampton, J., Miyabe, N., 2002. Application of a habitat-based model to estimate effective longline fishing effort and relative abundance of Pacific bigeye tuna (*Thunnus obesus*). Fish Oceangr. 11, 143–155.

Bigelow, K.A., Michael, K., Musyl, M.K., Poisson, F., Kleiber, P., 2006. Pelagic longline gear depth and shoaling. Fish. Res. 77, 173–183.

Bjordal, A., Lokkeborg, S., 1996. Longlining. In: Fishing New Book, 1st ed. Blackwell, Oxford, 156 pp.

Boggs, C.H., 1992. Depth, capture time, and hooked longevity of longline-caught pelagic fish: timing bites of fish with chips. Fish. Bull. 90, 642–658.

Campbell, R., 1997. Domestic longline fishing methods and the catch of tunas and non-target species off north-eastern Queensland (1st survey – October to December, 1995). Report to the Australian Fisheries Management Authority, Canberra, 70 pp.

Campbell, R., 2004. CPUE standardization and the construction of indices of stock abundance in a spatially varying fishery using general linear models. Fish. Res. 70, 209–227.

Gerasimov, V.G., 1971. Technique and organization in the search of commercial tuna stock in the Indian Ocean from ships of SRTM type (Tekhnika i organizatsiya poiska skoplenij tuntsov v Indijskom okeane s sudov tipa SRTM). In: Proceedings of AzCherNIRO (Trudy AzCherNIRO). Kerch. 32, pp. 15–22 (In Russian).

Gong, Y., Lee, J-U., Kim, Y-S., Yang, W-S., 1989. Fishing efficiency of Korean regular and deep longline gears and vertical distribution of tunas in the Indian Ocean. Bull. Kor. Fish. Soc. 22, 86–94.

Goodyear, C.P., Die, D., Kerstetter, D.W., Olson, D.B., Prince, E., Scott, G.P., 2003. Habitat standardization of CPUE indices: research needs. Coll. Vol. Sci. Pap. ICCAT 55 (2), 613–623.

Hanamoto, E., 1974. Fishery oceanography of bigeye tuna I. Depth of capture by tuna longline gear in the eastern tropical Pacific Ocean. La Mer 13, 58–71.

Hanamoto, E., 1987. Effect of oceanographic environment on bigeye tuna distribution. Bull. Jpn. Soc. Fish. Oceanogr. 51, 203–216.

Hoeting, J.A., Raftery, A.E., Madigan, D., 1996. A method for simultaneous variable selection and outlier identification in linear regression. J. Comput. Statist. 22, 251–271.

Hinton, M.G., Nakano, H., 1996. Standardizing catch and effort statistics using physiological, ecological, or behavioural constraints and environmental data, with an application to blue marlin (*Makaira nigricans*) catch and effort data from the Japanese longline fisheries in the Pacific. Inter-Am. Trop. Tuna Comm. 21, 169–200.

Kuznetsov, V.P., 1969. Setting of the tuna longline to defined layer (Postanovka tuntsovogo yarusa na zadannyj gorizont). In: Proceedings of AtlantNIRO. AtlantNIRO, Kaliningrad, pp. 179–187 (In Russian).

Lebreton, J.-D., Burnham, K.P., Clobert, J., Anderson, D.R., 1992. Modeling survival and testing biological hypotheses using marked animals: a unified approach with case studies. Ecol. Monographs 62, 67–118.

Lee, J.H., Lee, C.W., Cha, B.J., 2005. Dynamic simulation of tuna longline gear using numerical methods. Fish. Sci. 71, 1287–1294.

Madec, G., Delecluse, P., Imbard, M., Levy, C., 1999. OPA 8.1 Ocean General Circulation Model reference manual. Notes du Pôle de Modélisation, Institut Pierre Simon Laplace (IPSL), France, 11, 91 pp.

Maunder, M., Hinton, M.G., Bigelow, K.A., Langley, A.D., 2006a. Developing indices of abundance using habitat data in a statistical framework. Bull. Mar. Sci. 79, 545–559.

Maunder, M., Punt, A., 2004. Standardizing catch and effort data: a review of recent approaches. Fish. Res. 70, 141–149.

Maunder, M., Sibert, J.R., Fonteneau, A., Hampton, J., Kleiber, P., Harley, S.J., 2006b. Interpreting catch per unit effort data to assess the status of individual stocks and communities. ICES J. Mar. Sci. 63, 1373–1385.

Menkes, C., Vialard, J., Kennan, S., Boulanger, J-P., Madec, G., 2006. A modelling study of the three dimensional heat budget of tropical instability waves in the equatorial Pacific. J. Phys. Oceanogr. 36 (5), 847–865.

Miyamoto, Y., Uchida, K., Orii, R., Wen, Z., Shiode, D., Kakihara, T., 2006. Three-dimensional underwater shape measurement of tuna longline using ultrasonic positioning system and ORBCOMM buoy. Fish. Sci. 72, 63–68.

Mizuno, K., Okazaki, M., Okamura, H., 1997. Estimation of underwater shape of tuna longline by using micro-BTs. Bull. Nat. Res. Inst. Far Seas Fish. 34, 1–24.

Mizuno, K., Okazaki, M., Miyabe, N., 1998. Fluctuation of longline shortening rate and its effect on underwater longline shape. Bull. Nat. Res. Inst. Far Seas Fish. 35, 155–164.

Nakano, H., Okazaki, M., Okamoto, H., 1997. Analysis of catch depth by species for tuna longline fishery based on catch by branch lines. Bull. Nat. Res. Inst. Far Seas Fish. 34, 43–62.

Nishi, T., 1990. The hourly variations of the depth of hooks and the hooking depth of yellowfin tuna (*Thunnus albacares*), and bigeye tuna (*Thunnus obesus*), of tuna longline in the eastern region of the Indian Ocean. Mem. Fac. Fish. Kagoshima Univ. 39, 81–98.

Offcoast Inc., 1997. Modeling gear configuration of longlines. Report No.:OCI-97-202, 201 Hamakua Drive, Suite C-107, Kailua, HI 96734, USA, 7 pp.

Okamura, H., Mizuno, K., Okazaki, M., 1998. Estimation of the distance between the floats of longline on the sea using the GPS. Bull. Nat. Res. Inst. Far Seas Fish. 35, 165–175.

Okazaki, M., Mizuno, K., Watanabe, T., Yanagi, S., 1997. Improved model of micro bathythermograph system for tuna longline boats and its application to fisheries oceanography. Bull. Nat. Res. Inst. Far Seas Fish. 34, 25–41.

Richards, L.J., Schnute, J.T., 1986. An experimental and statistical approach to the question: is CPUE an index of abundance? Can. J. Fish. Aquat. Sci. 43 (6), 1214–1227.

Satoh, K., Kusaga, I., Takeda, S., Sakai, H., Inoue, K., 1990. Tuna long-line tests using monofilament Nylon. Nippon Suisan Gakkaishi 56 (10), 1605–1609 (in Japanese with English Abstract).

Suzuki, Z., Warashina, Y., Kishida, M., 1977. The comparison of catches by regular and deep tuna longline gears in the western and central equatorial Pacific. Bull. Far Seas Fish. Res. Lab. 15, 51–89.

Takeuchi, Y., 2001. Is historically available hooks-per-basket information enough to standardize actual hooks-per-basket effects on CPUE? Preliminary simulation approach. ICCAT Coll. Vol. Sci. Pap. 53, 356–364.

Venables, W.N., Ripley, B.D., 2002. Modern Applied Statistics with S, 4th ed. Springer-Verlag, New York, p. 495.

Ward, P., Hindmarsh, S., 2007. An overview of historical changes in the fishing gear and practices of pelagic longliners, with particular references to Japan's pacific fleet. Rev. Fish. Biol. Fish. 17 (4), 501–516.

Ward, P., Myers, R.A., 2005. Inferring the depth distribution of catchability for pelagic fishes and correcting for variations in the depth of longline fishing gear. Can. J. Fish. Aquat. Sci. 62, 1130–1142.

Ward, P., Myers, R.A., Blanchard, W., 2004. Fish lost at sea: the effect of soak time on pelagic longline catches. Fish. Bull. 102, 179–195.

Yoshihara, T., 1951. Distribution of fishes caught by the long line. II. Vertical distribution. Bull. Jpn. Soc. Sci. Fish. 16, 370–374.

Yoshihara, T., 1954. Distribution of catches of tuna longline. IV. On the relation between K and φ_0 with a table and diagram. Bull. Jpn. Soc. Sci. Fish. 19, 1012–1014.